Structure and dynamics of Rh surfaces

Jianjun Xie and Matthias Scheffler
Fritz-Haber-Institut der Max-Planck-Gesellschaft, Faradayweg 4-6, D-14195 Berlin-Dahlem, Germany
(Received 7 August 1997; revised manuscript received 8 October 1997)

Lattice relaxations, surface phonon spectra, surface energies, and work functions are calculated for Rh(100) and Rh(110) surfaces using density-functional theory and the full-potential linearized augmented plane-wave method. Both the local-density approximation and the generalized gradient approximation to the exchange-correlation functional are considered. The force constants are obtained from the directly calculated atomic forces, and the temperature dependence of the surface relaxation is evaluated by minimizing the free energy of the system. The anharmonicity of the atomic vibrations is taken into account within the quasiharmonic approximation. The importance of contributions from different phonons to the surface relaxation is analyzed. [S0163-1829(98)06007-X]

I. INTRODUCTION

Experimentally, the structure of a solid surface can be determined by low-energy electron diffraction (LEED),[1] ion scattering,[2] x-ray diffraction,[3] and helium-atom scattering.[3] Surface phonons can be measured by high-resolution electron energy-loss spectroscopy[4] (EELS) and inelastic helium-atom scattering.[5] It is well understood that the first interlayer separation of metal surfaces is typically contracted at room temperature,[6] and only few exceptions to this ''rule'' have been discovered so far. Due to the anharmonicity of the interatomic potentials, both the surface interlayer spacing and the bulk lattice constant depend on temperature. Furthermore, because of lower symmetry, the anharmonicity at the surface is expected to be more significant than that in the bulk.

First-principles calculations of lattice relaxations[6–11] and surface phonons for metals[12–15] typically employ the density-functional theory (DFT).[16] In most previous work, the equilibrium geometry was determined by minimizing the total energy of the system (we will call this the ''static equilibrium''). We note that the surface structure obtained in this way corresponds to $T=0$ K and neglects the effects of zero-point vibrations. For example, with respect to the latter, we note that for the crystal bulk, zero-point vibrations give rise to an increase of the lattice constant by about 0.2–0.5%, compared to the geometry determined by the total-energy minimum.[17,18] Starting from the ''static equilibrium'' geometry, surface phonons were calculated either directly (using the supercell approach)[12–14] or by applying density-functional perturbation theory.[15,19]

At finite temperature, the equilibrium geometry is determined by the minimum of the free energy, which, in addition to the total energy, includes the contribution from lattice vibrations. Typically this gives rise to a lattice expansion, but it is also possible that contractions occur.[18] Because anharmonicity is more pronounced at the surface than in the bulk, an increased interlayer of spacing of the top layer, d_{12}, is to be expected.[20,21] Recently, Narasimhan and Scheffler[22] and Cho and Scheffler[23] performed a theoretical study of the thermal expansion of Ag(111) and Rh(100). The free energy was calculated by including the contribution of phonons in the quasiharmonic approximation.[18,24] The temperature dependence of d_{12} was obtained by minimizing the free energy of the considered slab with respect to d_{12}. In these studies,[22,23] as a first approximation, only the top layer was allowed to vibrate as a whole parallel and perpendicular to the surface. The effective vibrational ''modes'' considered in these works correspond to modes at the Brillouin zone center for the top layer vibrating on a rigid substrate. No information about the true surface phonon spectrum was obtained, and thus, not even an attempt was made to discuss how a good-quality summation over the phonon Brillouin zone may affect the result. In fact, a better treatment is quite elaborate as it requires the diagonalization of the dynamical matrix of the whole slab. In order to improve on previous calculations,[23] we present in this paper a theoretical study of the structure and dynamics of Rh(100) and Rh(110) surfaces by including vibrations of the whole slab. The interplanar force constants are obtained from the directly calculated atomic forces using the full-potential linearized augmented plane-wave (FP-LAPW) method.[25,26] It has been shown[12,13] that the surface phonon modes for wave vectors at high-symmetry points of the surface Brillouin zone (SBZ) can be determined from the knowledge of interplanar force constants. In the present work, these force constants and the corresponding surface phonons are calculated as a function of the interlayer spacing at the surface. The temperature dependence of surface relaxation is then determined by minimizing the free energy within the quasiharmonic approximation. Contributions from different phonon modes to the vibrational free energy will be examined. In Sec. II, we will describe some details of the calculation method. The results are presented in Sec. III.

II. METHOD OF CALCULATION

A. General theory

We consider a crystal slab consisting of a finite number of atomic layers perpendicular to the z direction, and of infinite extension in the x and y directions. In the quasiharmonic approximation, the free-energy function of the considered system can be written as[18]

$$F(\{d_{ij}\},T)=\Phi(\{d_{ij}\})+F_{\rm vib}(\{d_{ij}\},T)$$
$$=\Phi(\{d_{ij}\})+k_BT\times\sum_{\mathbf{q}_{||}}\sum_{p=1}^{3N}\ln\left\{2\sinh\left(\frac{\hbar\omega_p(\mathbf{q}_{||},d_{ij})}{2k_BT}\right)\right\},\qquad(2.1)$$

where Φ is the static total energy which can be obtained by first-principles calculations, k_B and $\hbar$ are Boltzmann and Planck constants, and $\{d_{ij}\}$ is the set of interlayer distances, d_{12}, d_{23}, . . . , between layers 1 and 2, 2 and 3, etc. The vibrational free energy is denoted as $F_{\rm vib}$, and $\omega_p(\mathbf{q}_{||},\{d_{ij}\})$ is the frequency of the pth mode for a given wave vector $\mathbf{q}_{||}$, evaluated at the geometry defined by $\{d_{ij}\}$; and N is the number of atoms in the slab. Anharmonicity of the interatomic potentials is included in this description because Φ and the vibrational frequencies ω_p depend on the interlayer distances $\{d_{ij}\}$. The free energy and the equilibrium distances $\{d_{ij}^0\}$ at a given temperature are determined by the minimum of $F(\{d_{ij}\},T)$ with respect to $\{d_{ij}\}$.

In the present work, we have calculated the vibrational frequencies and the corresponding free energy using the slab model[27] and the density-functional theory. We expand the static total energy Φ of the system in a Taylor series:

$$\Phi=\Phi_0+\sum_{\mathbf{l},\alpha}\phi_\alpha(\mathbf{l})u_\alpha(\mathbf{l})+\frac{1}{2}\sum_{\mathbf{l},\alpha}\sum_{\mathbf{l}',\beta}\phi_{\alpha\beta}(\mathbf{l},\mathbf{l}')u_\alpha(\mathbf{l})u_\beta(\mathbf{l}')+\cdots,\qquad(2.2)$$

where $u_\alpha(\mathbf{l})$ is the α component ($\alpha=x,y,z$) of the displacement of the $\mathbf{l}$th atom from its mean position $\mathbf{R}_0(\mathbf{l})$ (taking the thermal expansion of the lattice into account). The instantaneous position of an atom is given by $\mathbf{r}(\mathbf{l})=\mathbf{R}_0(\mathbf{l})+\mathbf{u}(\mathbf{l})$. We consider here that the monatomic lattice, and the set of integers $\mathbf{l}=(l_1,l_2,l_3)$, which specify a particular atom, have the following meaning: l_3 labels the crystal planes lying parallel to the surface, and l_1,l_2 specify the points in the two-dimensional lattice which spans a plane. In the quasiharmonic approximation the equations of motion are

$$M\frac{d^2}{dt^2}u_\alpha(\mathbf{l})=-\sum_{\mathbf{l}',\beta}\phi_{\alpha\beta}(\mathbf{l},\mathbf{l}')u_\beta(\mathbf{l}'),\qquad(2.3)$$

where M is the atomic mass, $\phi_{\alpha\beta}(\mathbf{l},\mathbf{l}')$ is the force constant which is defined by

$$\phi_{\alpha\beta}(\mathbf{l},\mathbf{l}')=\left(\frac{\partial^2\Phi}{\partial u_\alpha(\mathbf{l})\partial u_\beta(\mathbf{l}')}\right)_0.\qquad(2.4)$$

The subscript ''0'' in Eq. (2.4) indicates that the force constants $\phi_{\alpha\beta}(\mathbf{l},\mathbf{l}')$ are to be evaluated at the mean positions of the atoms, rather than at the positions of the static equilibrium. Due to the two-dimensional translational property of the slab, the normal-mode solutions to Eq. (2.3) have the form[27]

$$u_\alpha(\mathbf{l})=M^{-1/2}Q_0\zeta_\alpha(l_3)\exp\{i[\mathbf{q}_{||}\cdot\mathbf{R}_{0||}(\mathbf{l}_{||})+\mathbf{q}_{||}\cdot\mathbf{R}_{0||}(l_3)-\omega t]\},\qquad(2.5)$$

where Q_0 is the vibrational amplitude, $\zeta_\alpha(l_3)$ is a polarization vector which will turn out to be the eigenvectors of the dynamical matrix, and ω is the vibrational frequency. Following the notation of Ref. 27, we have $\mathbf{q}_{||}=(q_x,q_y)$, $\mathbf{R}_{0||}=(x,y)$, $\mathbf{R}_{0||}(\mathbf{l})=\mathbf{R}_{0||}(\mathbf{l}_{||})+\mathbf{R}_{0||}(l_3)$, $\mathbf{l}_{||}=(l_1,l_2)$. Insertion of Eq. (2.5) into Eq. (2.3) leads to the eigenvalue equation

$$\sum_{l_3',\beta}D_{\alpha\beta}(l_3,l_3';\mathbf{q}_{||})\zeta_\beta(l_3';\mathbf{q}_{||})=\omega^2(\mathbf{q}_{||})\zeta_\beta(l_3;\mathbf{q}_{||}),\qquad(2.6)$$

where the elements of the dynamical matrix are defined by

$$D_{\alpha\beta}(l_3,l_3';\mathbf{q}_{||})=\frac{1}{M}\sum_{\mathbf{l}_{||}'}\phi_{\alpha\beta}(l_3,l_3',\mathbf{l}_{||}'-\mathbf{l}_{||})\times\exp\{i\mathbf{q}_{||}\cdot[R_{0||}(\mathbf{l}_{||}'-\mathbf{l}_{||})+R_{0||}(l_3')-R_{0||}(l_3)]\}.\qquad(2.7)$$

TABLE I. Surface relaxations $\Delta d_{12}/d_0$ and $\Delta d_{23}/d_0$, work function ϕ (eV), and surface energies σ (eV/atom) for Rh(100) and Rh(110) surfaces obtained by different calculations and experiments. The results correspond to $T=0$ K, and none of the theoretical values includes the effect of zero-point vibrations.

		$\Delta d_{12}/d_0$	$\Delta d_{23}/d_0$	ϕ	σ
Rh(100)	LDA (Ref. 6)	−3.5%		5.25	1.27
	LDA (Ref. 11)	−3.8%	+0.7%		1.44
	LDA (Ref. 23)	−3.0%	−0.2%	5.26	1.29
	GGA (Ref. 23)	−2.8%	−0.1%	4.92	1.04
	LDA	−3.3%	−0.2%	5.30	1.23
	GGA	−3.0%	−0.1%	4.91	0.99
	experiment	+0.5±1.0% (Ref. 31)	0±1.5% (Ref. 31)	4.65 (Ref. 32)	1.12 (Ref. 33)
	experiment	−1.16±1.6% (Ref. 34)	0±1.6% (Ref. 34)		
Rh(110)	LDA (Ref. 35)	−10.2%	+2.5%	4.99	1.92
	LDA (Ref. 11)	−9.8%	+2.6%		2.05
	LDA	−9.9%	+2.0%	4.94	1.85
	GGA	−9.2%	+2.1%	4.59	1.43
	experiment	−6.9±1.0% (Ref. 36)	+1.9±1.0% (Ref. 36)	4.98 (Ref. 37)	1.27 (Ref. 38)

TABLE II. Interplanar force constants of Rh(100) coupling the surface layer to other layers for wave vectors at $\bar{\Gamma}$, $\bar{X}$, and $\bar{M}$ at $\Delta d_{12}/d_0 = -3.0\%$, $\Delta d_{23}/d_0 = -0.1\%$. The units are 10^4 dyn/cm. The corresponding interplanar force constants for the interior layers of the slab are also shown for comparison. The indices $(\alpha\beta)$ and the arguments (l_3, l_3') of $\phi^p_{\alpha\beta}(l_3, l_3')$ are combined as $(l_3\alpha, l_3'\beta)$. Matrix elements not listed are zero by symmetry.

$(l_3\alpha, l_3'\beta)$	Surface	Interior	$(l_3\alpha, l_3'\beta)$	Surface	Interior
			$\mathbf{q}_{\parallel}=\bar{\Gamma}$		
$(1x, 2x)$	−4.89	−4.92	$(1x, 3x)$	−0.03	−0.30
$(1z, 2z)$	−8.34	−7.65	$(1z, 3z)$	−1.45	−1.84
			$\mathbf{q}_{\parallel}=\bar{X}$		
$(1x, 1x)$	14.65	26.23	$(1x, 3x)$	0.53	0.39
$(1y, 1y)$	6.34	10.18	$(1y, 3y)$	−0.08	0.03
$(1z, 1z)$	10.15	17.07	$(1z, 3z)$	−0.57	−0.70
$(1x, 2z)$	−6.42	−5.46	$(1z, 2x)$	−5.41	−5.46
			$\mathbf{q}_{\parallel}=\bar{M}$		
$(1x, 1x)$	14.60	23.70	$(1x, 3x)$	−0.50	−0.72
$(1z, 1z)$	15.01	18.49	$(1z, 3z)$	−0.88	−0.59
$(1x, 2y)$	−2.59	−2.73	$(1y, 2x)$	−2.59	−2.73

TABLE III. Interplanar force constants for Rh(110) at $\bar{\Gamma}$, $\bar{X}$, $\bar{Y}$, and $\bar{S}$ at $\Delta d_{12}/d_0 = -9.2\%$, $\Delta d_{23}/d_0 = 2.1\%$. The units are 10^4 dyn/cm. The corresponding interplanar force constants for the interior layers of the slab are also shown for comparison. The indices $(\alpha\beta)$ and the arguments (l_3, l_3') of $\phi^p_{\alpha\beta}(l_3, l_3')$ are combined as $(l_3\alpha, l_3'\beta)$. Matrix elements not listed are zero by symmetry.

$(l_3\alpha, l_3'\beta)$	Surface	Interior	$(l_3\alpha, l_3'\beta)$	Surface	Interior
			$\mathbf{q}_{\parallel}=\bar{\Gamma}$		
$(1x, 2x)$	−5.13	−4.30	$(1x, 3x)$	0.31	−0.86
$(1y, 2y)$	−7.88	−7.14	$(1y, 3y)$	0.15	−0.14
$(1z, 2z)$	−3.95	−3.55	$(1z, 3z)$	−6.87	−4.44
			$\mathbf{q}_{\parallel}=\bar{X}$		
$(1x, 1x)$	13.52	25.40	$(1x, 3x)$	0.71	0.62
$(1y, 1y)$	9.51	17.24	$(1y, 3y)$	−0.07	−0.96
$(1z, 1z)$	13.68	16.56	$(1z, 3z)$	−5.88	−3.61
$(1x, 2z)$	−1.77	−3.09	$(1z, 2x)$	−3.48	−3.09
			$\mathbf{q}_{\parallel}=\bar{Y}$		
$(1x, 1x)$	5.69	10.81	$(1x, 3x)$	−0.49	0.11
$(1y, 1y)$	9.11	20.50	$(1y, 3y)$	1.74	1.08
$(1z, 1z)$	13.68	18.12	$(1z, 3z)$	−5.78	−3.67
$(1y, 2z)$	−5.52	−5.81	$(1z, 2y)$	−5.52	−5.81
			$\mathbf{q}_{\parallel}=\bar{S}$		
$(1x, 1x)$	13.83	24.16	$(1x, 3x)$	1.74	0.94
$(1y, 1y)$	10.21	17.81	$(1y, 3y)$	0.76	0.25
$(1z, 1z)$	13.66	16.44	$(1z, 3z)$	−6.20	−2.92
$(1x, 2y)$	−6.12	−5.23	$(1y, 2x)$	−4.23	−5.23

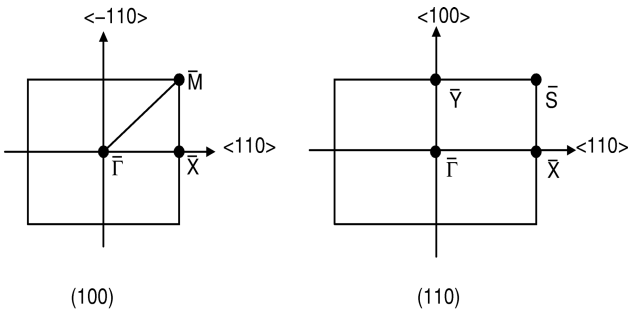

FIG. 1. Surface Brillouin zones for fcc (100) and (110) surfaces. High-symmetry points are indicated.

Once the force constants are obtained, the frequencies and polarization vectors for all modes in the slab for a given $\mathbf{q}_{\parallel}$ can be obtained by diagonalization of a $3N\times 3N$ matrix.

B. Density-functional theory calculation

In the present paper, the considered systems Rh(100) and Rh(110) are modeled by a periodic slab consisting of 7 layers of Rh and a vacuum region with the same thickness. We employ density-functional theory and the FP-LAPW method.[25,26] The exchange-correlation functional is treated by the local-density approximation[28] (LDA) as well as the generalized gradient approximation (GGA).[29] We first calculate the lattice relaxations, surface energies and work functions of Rh surfaces at $T=0$ K neglecting the influence of zero-point vibrations. The geometry is optimized by a damped molecular dynamics allowing the top two layers on both sides of the slab to relax. The remaining atoms are kept at the bulk lattice sites. The energy cutoff for the FP-LAPW

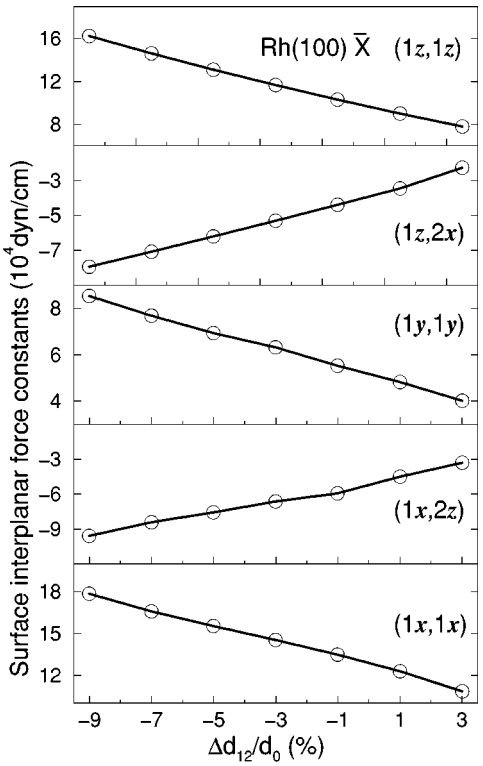

FIG. 2. Variation of the surface interplanar force constants at $\bar{X}$ with $\Delta d_{12}/d_0$ for Rh(100).

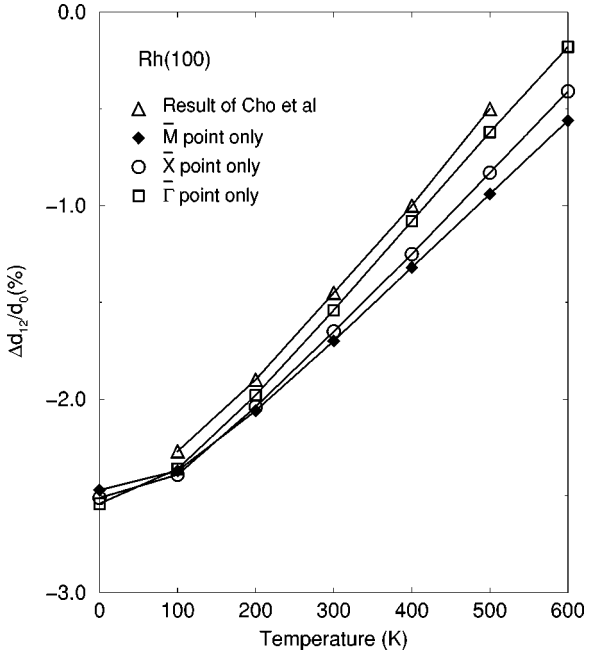

FIG. 3. Top-layer relaxation of Rh(100) as a function of temperature calculated in different approximations, i.e., including different vibration modes. The results of Cho and Scheffler (Ref. 23) are shown for comparison.

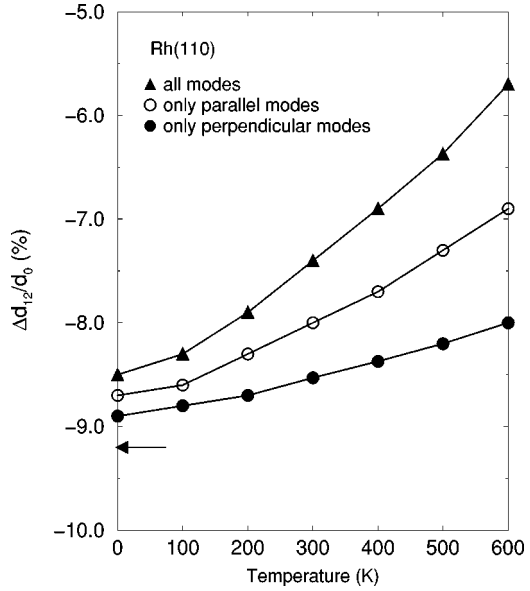

FIG. 5. Top-layer relaxation of Rh(110) as a function of temperature calculated by including the vibration modes at $\bar{\Gamma}$, $\bar{X}$, $\bar{Y}$, and $\bar{S}$. The contributions from vibrations parallel and perpendicular to the surface are displayed. The arrow points to the result obtained when vibrational contributions to the free energy are neglected completely.

basis is taken to be 15 Ry and for the wave functions inside the muffin-tin spheres angular momenta are taken into account up to $l_{\max}^{\mathrm{wf}}=8$. The cutoff energy for the potential is taken as $G^2=100$ Ry. For the $\mathbf{k}_{||}$ sampling, we use a uniform mesh of 15 points in the irreducible part of SBZ of the (1×1) surface displaced from $\bar{\Gamma}$.

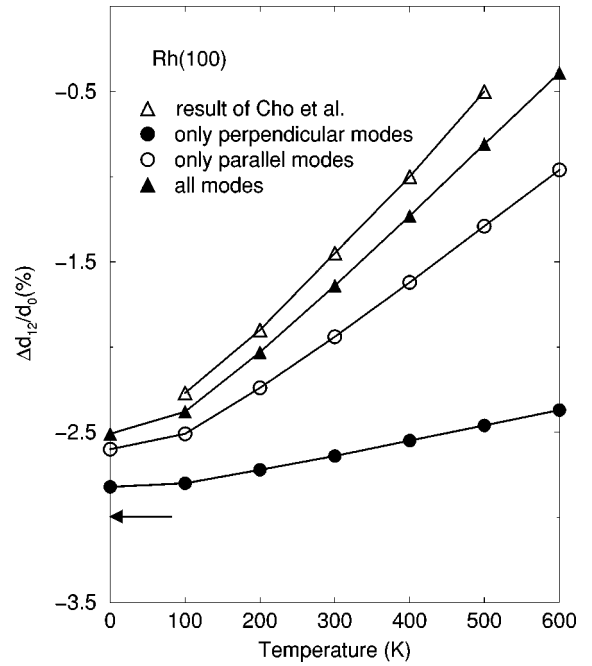

FIG. 4. Top-layer relaxation of Rh(100) as a function of temperature calculated by including the vibration modes at $\bar{\Gamma}$, $\bar{X}$, and $\bar{M}$. The contributions from vibration, parallel and perpendicular to the surface, are displayed. The arrow points to the result obtained when vibrational contributions to the free energy are neglected completely. The result of Cho and Scheffler (Ref. 23) are shown for comparison.

In order to calculate phonon frequencies of the slab, an extension of the ''frozen phonon'' method[12] is used. For a selected $\mathbf{q}_{||}$ in the surface Brillouin zone, we can calculate all the interplanar force-constant matrices by distorting the slab in an appropriate way. The obtained force constants allow us to set up the dynamical matrix and solve for the eigenvalues and eigenvectors of the system. The interplanar force constants coupling planes l_3 and l_3' are given by

$$\phi^p_{\alpha\beta}(l_3,l_3';\mathbf{q}_{||})=\sum_{\mathbf{l}_{||}'}\phi_{\alpha\beta}(l_3,l_3',\mathbf{l}_{||}'-\mathbf{l}_{||})\times\exp[i\mathbf{q}_{||}\cdot\mathbf{R}_{0||}(\mathbf{l}_{||}'-\mathbf{l}_{||})]\,. \tag{2.8}$$

In the harmonic or quasiharmonic approximation, the interplanar force constants $\phi^p_{\alpha\beta}(l_3,l_3';\mathbf{q}_{||})$ are related to the forces by

TABLE IV. Calculated surface phonon frequencies ν for Rh(100) and Rh(110) corresponding to surface relaxation at $T=300$ K. Units are in THz.

Rh(100)				Rh(110)					
$\bar{X}$		$\bar{M}$		$\bar{X}$		$\bar{Y}$		$\bar{S}$	
ν	mode	ν	mode	ν	mode	ν	mode	ν	mode
2.97	S_1	4.44	S_1	3.44	S_1	2.50	S_1	3.54	S_1
3.36	S_4	4.50	L_1	3.54	S_2	2.62	S_2	3.66	S_2
3.42	S_2			5.13	S_7	3.65	S_3	3.78	S_3
5.40	S_6					4.52	S_5	5.26	S_7

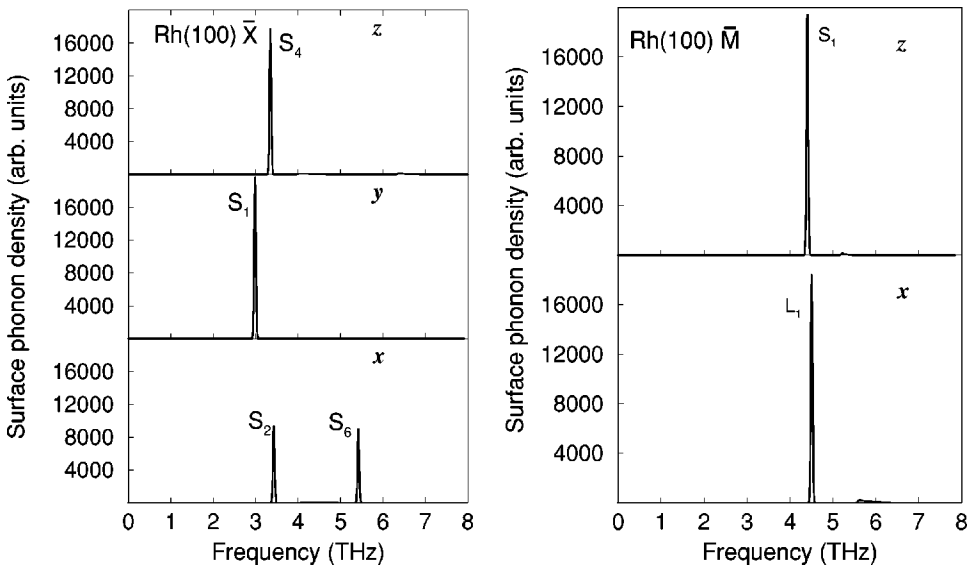

FIG. 6. Surface phonon density of states of Rh(100) for the wave vectors at $\bar{X}$ and $\bar{M}$ points in the surface Brillouin zone.

$$\phi^p_{\alpha\beta}(l_3,l_3';\mathbf{q}_{||}) = -\frac{\partial F_\alpha(l_3,\mathbf{q}_{||})}{\partial u_\beta(\mathbf{l}_{||},l_3')} \approx -\frac{\Delta F_\alpha(l_3,\mathbf{q}_{||})}{u_\beta(\mathbf{l}_{||},l_3')}, \tag{2.9}$$

where $\Delta F_\alpha(l_3,\mathbf{q}_{||})$ is the α component of the force difference at atomic layer l_3 under a distortion of layer l_3' in accordance with $\mathbf{q}_{||}$, $u_\beta(\mathbf{l}_{||},l_3')$ is the β component of atomic displacement at $(\mathbf{l}_{||},l_3')$. The displacement for other atoms in layer l_3' is given by

$$\mathbf{u}(\mathbf{l}_{||}',l_3') = \mathbf{u}(\mathbf{l}_{||},l_3')\exp[i\mathbf{q}_{||}\cdot\mathbf{R}_{0||}(\mathbf{l}_{||}'-\mathbf{l}_{||})]\,. \tag{2.10}$$

The dynamical matrix of Eq. (2.7) can then be written as

$$D_{\alpha\beta}(l_3,l_3';\mathbf{q}_{||}) = \frac{1}{M}\phi^p_{\alpha\beta}(l_3,l_3';\mathbf{q}_{||}) \times \exp\{i\mathbf{q}_{||}\cdot[\mathbf{R}_{0||}(l_3')-\mathbf{R}_{0||}(l_3)]\}\,. \tag{2.11}$$

In order to calculate the thermal expansion, we need to know the interplanar force constants as a function of the interlayer distance. In most cases, the thermal expansion of the lattice at the surface along the z direction is expected to be more significant than the expansion of the bulk lattice constant. The latter also defines the expansion of interatomic distance in the x-y plane. We therefore calculate the surface interplanar force constants as a function of d_{12}. Furthermore, we calculate the interplanar force constants for the crystal bulk. From all the interplanar force constants, the dynamical matrix (as a function of d_{12}) of the considered slab can be constructed. The surface relaxation $d_{12}(T)$ is then obtained by minimizing the free energy of the slab for various temperatures. For the phonon calculations it is important to use a significantly thicker slab than for the electronic structure calculations, in order to obtain a reliable description of surface modes, surface resonances, and the surface phonon density of states.[12,27] We therefore calculate the surface phonon spectra for Rh(100) and Rh(110) for a 201-layer thick slab.

III. RESULTS

For Rh bulk the theoretically obtained lattice constant (neglecting the zero-point vibrations) is $a^{\text{th}}=3.79$ Å for DFT-LDA and $a^{\text{th}}=3.83$ Å for DFT-GGA. The FP-LAPW parameters employed for these calculations are the same as those for the surface calculations stated in Sec. II B, except that for the bulk study we use a mesh of 72 **k** points in the irreducible part of the fcc Brillouin zone. The experimental value is $a^{\text{exp}}=3.80$ Å.[30] The surface properties of Rh are calculated with the theoretical bulk lattice constant. In Table I, we present the results of surface relaxations, work functions, and surface energies of Rh(100) and Rh(110) calculated via LDA and GGA neglecting the zero-point vibration. Results from other calculations and the experiments are also listed for comparison. The present reults are in good agreement with those of previous calculations.[6,11,23,35] In the following calculations of the surface dynamics, we will use the GGA. The surface interplanar force constant will be calculated as a function of d_{12}, while the interlayer spacing d_{23} is kept as the static equilibrium value.

The calculated interplanar force constants coupling the surface layer with other layers in the Rh(100) slab are given in Table II. Three high-symmetry surface wave vectors are considered (see Fig. 1): $\bar{\Gamma}$, $\bar{X}$, and $\bar{M}$. These results are obtained by distorting the slab around the zero-force geometry at $T=0$ K, and are given in Table I. The corresponding results for the interior of the slab are given as well. The interplanar force-constant matrices for the Rh(110) surface are given in Table III. Four wave vectors at $\bar{\Gamma}$, $\bar{X}$, $\bar{Y}$, and $\bar{S}$ points in the SBZ are considered (see Fig. 1). It is not surprising to see in Tables II and III that the intralayer part of the force constants $[\phi^p_{\alpha\beta}(1,1)]$ are most significantly changed at the surface compared to that in the bulk because of the truncation of the surface. At the same time, the interlayer part of the force constants at the surface $[\phi^p_{\alpha\beta}(1,l_3),l_3=2,3]$ are also modified due to the surface relaxations. For most of the matrix elements in Table III, there is a trend for an enhancement in magnitude for force con-

stants coupling the surface layer to its neighbors compared with the bulk force-constant matrix elements. This is in agreement with the findings of Al(110).[12]

Anharmonicity is included in our studies by calculating the force constants as a function of the interlayer distance d_{12}. Figure 2 shows the variation of the surface interplanar force constants at $\bar{X}$ point for Rh(100). It can be clearly seen that the interlayer force constants decrease monotonically as d_{12} changes from a 9% contraction to a 3% expansion. This ''softening'' of the force constants reflects the anharmonicity of the bond strength at this surface. We also note that the intralayer force constants of the second layer $\phi^p_{\alpha\beta}(2,2)$ are also significantly softened at the $\bar{X}$ point and $\bar{M}$ points for Rh(100), and at the $\bar{X}$, $\bar{Y}$, and $\bar{S}$ points for Rh(110), with the increase of d_{12}. While at $\bar{\Gamma}$, there are no intraplanar vibrations, the ''softening'' of $\phi^p_{\alpha\beta}(2,2)$ is already included in the surface interplanar force constant $\phi^p_{\alpha\beta}(1,2)$. In the present work, the changes of the intraplanar force constants for the second layer with d_{12} are taken into account.

Having obtained the force constants for different d_{12}, we calculate the phonon frequencies of the slab for each d_{12}. The temperature-dependent top-layer relaxations for Rh(100) and Rh(110) are determined by minimizing the free energy with respect to d_{12}. Figure 3 shows the variation of $\Delta d_{12}/d_0$ for Rh(100) with temperature in the case in which vibrations are calculated from different wave vectors $\mathbf{q}_{||}$ in SBZ. The results of Cho and Scheffler[23] are also given for comparison. It can be seen that when only the $\bar{\Gamma}$-point vibration is taken into account, the variation of $\Delta d_{12}/d_0$ with temperature is in close agreement with the results of Cho and Scheffler.[23] The small difference is due to the fact that only the top layer was allowed to vibrate in Ref. 23, while in the present work, vibrations of the whole slab are included. At low temperature (below 300 K), the vibrations from $\bar{\Gamma}$, $\bar{X}$, and $\bar{M}$ points contribute with similar importance to the surface expansion. The differences between the contributions of the different $\mathbf{q}_{||}$ vectors becomes significant at high temperature because of the different frequency distributions between $\bar{\Gamma}$, $\bar{X}$, and $\bar{M}$.

Using the ''frozen'' phonon method,[12,39,40] it is not practicable to get the phonon frequency for an arbitrary $\mathbf{q}_{||}$ point in SBZ. For phonons, in contrast to electrons, it is in fact acceptable to approximate the summation over the whole SBZ by the contributions from only the high-symmetry $\mathbf{q}_{||}$ points. The weights of $\bar{\Gamma}$, $\bar{X}$, and $\bar{M}$ are $\frac{1}{4}$, $\frac{2}{4}$, and $\frac{1}{4}$, respectively. Thus, the vibrational free energy is given by $F_{\mathrm{vib}} = \frac{1}{4}F_{\mathrm{vib}}(\bar{\Gamma}) + \frac{2}{4}F_{\mathrm{vib}}(\bar{X}) + \frac{1}{4}F_{\mathrm{vib}}(\bar{M})$. The temperature dependence of the top-layer relaxation for Rh(100) including all the vibrational contributions from $\bar{X}$, $\bar{M}$, and $\bar{\Gamma}$ is shown in Fig. 4. The arrow marks the result of the surface relaxation obtained when lattice vibrations (also zero-point effects) are neglected. We find that at low temperature the thermal expansion for Rh(100) is close to the result of Cho and Scheffler.[23] At 300 K, the top-layer relaxation is -1.64%, the value found in Ref. 23 is -1.45%. However, for higher temperature the thermal expansion will be overestimated if only the vibrations at Γ point are included. In general, our improved calculations confirm the conclusion of Cho and Scheffler.[23] The calculated surface thermal expansion coefficient is $\alpha_s = (d_{12})^{-1}(\partial d_{12}/\partial T) = 40.7\times10^{-6}\ \mathrm{K}^{-1}$ at $T=300$ K, which is 5.0 times larger than in the bulk [$\alpha_b = 8.2\times10^{-6}\ \mathrm{K}^{-1}$ (Ref. 41)]. Thus for Rh(100) the thermal expansion is clearly increased at the surface. The different contributions to the surface relaxation from vibrations parallel to the surface and perpendicular to the surface are also shown in Fig. 4. All the vibrational modes at $\bar{X}$, $\bar{\Gamma}$, and $\bar{M}$ are included. The results in Fig. 4 confirm that the parallel vibrations have a significantly larger influence on the surface thermal expansion than the perpendicular vibrations (z direction). This is in agreement with the findings and conclusions of Narasimhan and Scheffler,[22] and Cho and Scheffler.[23]

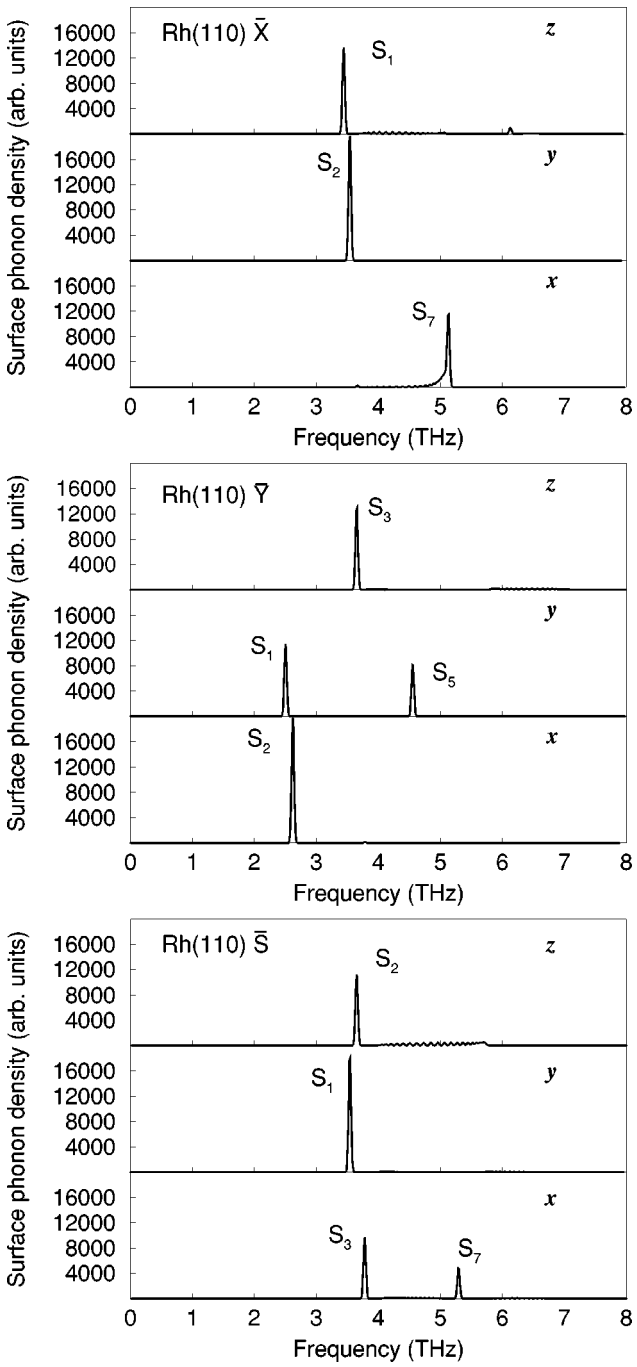

FIG. 7. Surface phonon density of states of Rh(110) for the wave vectors at $\bar{X}$, $\bar{Y}$, and $\bar{S}$ points in surface Brillouin zone.

We now turn to the more open (110) surface. The temperature dependence of the top-layer relaxation for Rh(110) is shown in Fig. 5. The vibrational free energy is calculated by summing over the wave vectors $\bar{\Gamma}$, $\bar{X}$, $\bar{Y}$, and $\bar{S}$ in the SBZ. These four points all have the same weight, therefore the vibrational free energy is given by $F_{\rm vib}=\frac{1}{4}[F_{\rm vib}(\bar{\Gamma})+F_{\rm vib}(\bar{X})+F_{\rm vib}(\bar{Y})+F_{\rm vib}(\bar{S})]$. Similar to Rh(100), the contribution to the thermal expansion of d_{12} from in-plane vibrations is larger than that from out-of-plane vibrations. At $T=300$ K we obtain the surface thermal expansion coefficient $\alpha_s=59.4\times10^{-6}$ K^{-1}, which is 7.2 times larger than the bulk thermal expansion coefficient. Comparing the thermal expansion coefficient of Rh(110) with that of Rh(100), we find that Rh(110) exhibits more significant anharmonicity than Rh(100). The top-layer relaxation is $\Delta d_{12}/d_0=-7.4\%$ at $T=300$ K, which is close to the result of a room-temperature LEED analysis,[36] which gave a value of $\Delta d_{12}/d_0=-6.9\%$. The surface relaxation obtained when just the total energy is minimized is noticeably different, namely $\Delta d_{12}/d_0=-9.2\%$.

In Table IV, we present the calculated surface phonon frequencies corresponding to the surface relaxation at $T=300$ K. The local density of states is obtained from

$$D_{\mathbf{q}_{||},\alpha}(\omega)=\sum_p \delta(\omega-\omega_p)|\zeta_\alpha(1,\mathbf{q}_{||}p)|^2, \qquad (3.1)$$

where $\zeta_\alpha(1,\mathbf{q}_{||}p)$ is the surface layer polarization vector for the pth normal mode of the slab with respect to wave vector $\mathbf{q}_{||}$, α denotes x,y, and z. The calculated surface phonon densities of states are shown in Figs. 6 and 7. Different plots correspond to different polarizations. At the $\bar{M}$ point for Rh(100) (Fig. 6), results for y polarization are identical to those for the x polarization due to symmetry. It can be seen that in all cases (Figs. 6 and 7), the surface modes are strongly localized at the surface and are well separated from the bulk modes. Thus it should be possible to identify them in EELS or He scattering experiments. It is these localized surface phonons that are most sensitive to the surface relaxations, and hence govern the anharmonic thermal expansion at the surface. It can be seen in Figs. 6 and 7 that there are more localized surface phonon modes polarized in x and y directions than in the z direction. This is one of the reasons why the parallel vibrations give a more important contribution to the thermal expansion (see Figs. 4 and 5).

IV. SUMMARY

In conclusion, we have used a full-potential FP-LAPW method to investigate the surface structures and surface phonon spectra of Rh(100) and Rh(110) surfaces. We studied the thermal expansion by taking anharmonicity into account within the quasiharmonic approximation. It is found that different phonons give different contributions to the surface relaxation in the high-temperature range (higher than 300 K). The surface thermal expansion coefficients calculated by including all the high-symmetry points in the surface Brillouin zone are 40.7×10^{-6} K^{-1} for Rh(100) and 59.4×10^{-6} K^{-1} for Rh(110) at $T=300$ K, which are 5.0 and 7.2 times larger than that of the bulk, respectively. The obtained surface relaxations of Rh(100) and Rh(110) at $T=300$ K are in agreement with the experimental measurements at room temperature. The calculated results confirm that the in-plane vibrations give a more important contribution to surface thermal expansion than the out-of-plane vibrations.

ACKNOWLEDGMENT

One of the authors (J.J. Xie) would like to acknowledge financial support from the Alexander von Humboldt Foundation in Germany.

[1] M.A. van Hove, W.H. Weinberg, and C.M. Chan, *Low Energy Electron Diffraction* (Springer-Verlag, Berlin, 1986).
[2] C. Varlas, in *Structures and Dynamics of Surfaces I*, Vol. 41 of *Topics in Current Physics*, edited by W. Schommers and P. von Blankenhagen (Springer, New York, 1986), p. 111.
[3] K.H. Rieder, in *Structure and Dynamics of Surfaces I* (Ref. 2), p. 17; J. Als-Nielsen, in *Structure and Dynamics of Surfaces II*, Vol. 43 of *Topics in Current Physics*, edited by W. Schommers and P. von Blankenhagen (Springer, New York, 1987), p. 181.
[4] H. Ibach and D.L. Mills, *Electron Energy Loss Spectroscopy and Surface Vibrations* (Academic Press, New York, 1982).
[5] J.P. Toennies, J. Vac. Sci. Technol. A **5**, 440 (1987); *Proceedings of the Solvay Conference on Surface Science*, edited by F. de Wette (Springer, Heidelberg, 1988).
[6] M. Methfessel, D. Hennig, and M. Scheffler, Phys. Rev. B **46**, 4816 (1992).
[7] Th. Rodach, K.P. Bohnen, and K.M. Ho, Surf. Sci. **286**, 66 (1993).
[8] P.J. Feibelman and D.R. Hammann, Surf. Sci. **234**, 377 (1990).
[9] J. Redinger, P. Weinberger, H. Erschbaumer, R. Podloucky, C.L. Fu, and A.J. Freeman, Phys. Rev. B **44**, 8288 (1991).
[10] I. Morrison, D.M. Bylander, and L. Kleinman, Phys. Rev. Lett. **71**, 1083 (1993).
[11] A. Eichler, J. Hafner, J. Furtmueller, and G. Kresse, Surf. Sci. **346**, 300 (1996).
[12] K.M. Ho and K.P. Bohnen, Phys. Rev. Lett. **56**, 934 (1986); Phys. Rev. B **38**, 12 897 (1988).
[13] K.P. Bohnen and K.M. Ho, Surf. Sci. Rep. **19**, 99 (1993).
[14] K.-P. Bohnen, A. Eichler, and J. Hafner, Surf. Sci. **368**, 222 (1996).
[15] A.G. Eguiluz, A.A. Maradudin, and R.F. Wallis, Phys. Rev. Lett. **60**, 309 (1988).
[16] For a review of density-functional theory, see *Theory of the Inhomogeneous Electron Gas*, edited by S. Lundqvist and N.H. March (Plenum, New York, 1983).
[17] V.L. Morruzi, J.F. Janak, and A.R. Williams, *Calculated Electronic Properties of Metals* (Pergamon, New York, 1978).
[18] S. Biernacki and M. Scheffler, Phys. Rev. Lett. **63**, 290 (1989).
[19] P. Pavone, K. Karch, O. Schütt, W. Windl, D. Strauch, P. Giannozzi, and S. Baroni, Phys. Rev. B **48**, 3156 (1993).
[20] Y. Cao and E.H. Conrad, Phys. Rev. Lett. **64**, 44 (1990).
[21] P. Statiris, H.C. Lu, and T. Gustafsson, Phys. Rev. Lett. **72**, 3574 (1994).

[22] S. Narasimhan and M. Scheffler, Z. Phys. Chem. (Munich) **202**, 253 (1997).
[23] J.H. Cho and M. Scheffler, Phys. Rev. Lett. **78**, 1299 (1997).
[24] R.E. Allen and F.W. de Wette, Phys. Rev. **179**, 873 (1969).
[25] P. Blaha, K. Schwarz, P. Dufek, and R. Augustyn, WIEN95, Technical University of Vienna, 1995. [Improved and updated Unix version of the original copyrighted WIEN code, which was published by P. Blaha, K. Schwarz, P. Sorantin, and S.B. Trickey, in Comput. Phys. Commun. **59**, 399 (1990)].
[26] B. Kohler, S. Wilke, M. Scheffler, R. Kouba, and C. Ambrosch-Draxl, Comput. Phys. Commun. **94**, 31 (1996).
[27] R.E. Allen, G.P. Alldredge, and F.W. de Wette, Phys. Rev. B **4**, 1648 (1971).
[28] J.P. Perdew and Y. Wang, Phys. Rev. B **45**, 13 244 (1992).
[29] J.P. Perdew, J.A. Chevary, S.H. Vosko, K.A. Jackson, M.R. Pederson, D.J. Singh, and C. Fiolhais, Phys. Rev. B **46**, 6671 (1992).
[30] C. Kittel, *Introduction to Solid State Physics*, 6th ed. (John Wiley & Sons, New York, 1986), p. 23.
[31] W. Oed, B. Dötsch, L. Hammer, K. Heinz, and K. Müller, Surf. Sci. **207**, 562 (1978).
[32] *American Institute of Physics Handbook*, 2nd ed. (McGraw-Hill, New York, 1963), pp. 9-8, 4-66, and 9-150.
[33] W.R. Tyson, Can. Metall. Q. **14**, 307 (1975).
[34] A.M. Begley, S.K. Kim, F. Jona, and P.M. Marcus, Phys. Rev. B **48**, 12 326 (1993).
[35] K. Stokbro, Phys. Rev. B **53**, 6869 (1996).
[36] W. Nichtl, N. Bickel, L. Hammer, K. Heinz, and K. Müller, Surf. Sci. **188**, L729 (1987).
[37] *CRC Handbook of Chemistry and Physics*, 67th ed. (Franklin, Elkins Park, PA, 1987), p. E-89.
[38] L.Z. Mezey and J. Giber, Jpn. J. Appl. Phys., Part 1 **21**, 1569 (1982).
[39] M.T. Yin and M.L. Cohen, Phys. Rev. B **26**, 3259 (1982).
[40] G.P. Srivastava, in *The Physics of Phonons* (Hilger, London, 1990), pp. 72–75.
[41] *CRC Handbook of Chemistry and Physics*, 76th ed. (Franklin, Elkins Park, PA, 1996), pp. 12–173.